# Numerical simulations for General-Relativistic Astrophysics

Probing Extreme Matter Through Numerical Relativity Simulations of Core-collapse Supernovae and Neutron Stars

**Harry Ho Yin, NG**

Supervisor: Prof. Tjonnie G.F.LI

This thesis submitted for the degree of
*Master of Philosophy in Physics*

Department of Physics
The Chinese University of Hong Kong
Hong Kong
31 July 2021

# Thesis Title

**Harry Ho Yin, NG**

## Abstract

abc

To mum and dad

# Declaration

I declare that.. í

# Acknowledgements

I want to thank...

# Abbreviations and Notation

Units : $c = G = M_{\odot} = 1$

| | |
|---|---|
| ADM | Arnowitt-Deser-Misner |
| BH | Black Hole |
| CCSNe | Core-Collapse Supernovae |
| NS | Neutron Star |

# Contents

# Chapter 1

# Introduction

# Chapter 2

# Formulations of Einstein Field Equations

## 2.1 Introduction

In the past decade, numerical relativity has matured to the state that stable and robust numerical calculations of the Einstein equations with or without matter has become feasible. The spacetimes of many interesting astrophysical systems such as stellar core collapses and binary systems of compact objects have been accurately modeled (see, e.g., [**XNS2**, **2018MNRAS.480.5272C**, **2019arXiv190811258C**] for recent reviews). In the standard $3 + 1$ decomposition of spacetime, the Einstein equations are split into a set of evolution equations and constraint equations. Nevertheless, one still has the freedom to choose the basic variables to evolve and reformulate the resulting systems of differential equations in order to improve the stability and accuracy of numerical simulations. This results in different formulations of numerical relativity, such as the so-called BSSN [**1995PhRvD..52.5428S**, **1999PhRvD..59b4007B**], CCZ4 [**2003PhRvD..67j4005B**], and Z4c [**2010PhRvD..81h4003B**] schemes, which are popular choices for numerical modelings. The practical applications of these different formulations are based on a free-evolution approach where the constraint equations are first solved for preparing the initial data and used subsequently only as an indicator to monitor the numerical accuracy during the evolution (see, e.g., [**2014PhRvD..89h4043M**]).

Alternatively, one can also formulate the Einstein equations based on a fully constrained-evolution approach where the constraint equations are solved and fulfilled to within the discretization errors during the evolution. Despite the fact that a constrained-evolution approach is theoretical appealing, such an approach is not popular among numerical relativists since solving the elliptic-type constraint equations during the evolution is generally computational expensive. In contrast to the active development and applications of free-evolution formulations, the last proposed constrained formulation of the Einstein equations was already 17 years ago due to Bonazzola *et al.* [**2004PhRvD..70j4007B**] in 2004. The fully constrained-evolution formulation of Bonazzola *et al.* [**2004PhRvD..70j4007B**] has been employed to simulate pure gravitational wave spacetime [**2004PhRvD..70j4007B**], and also an oscillating neutron star by ignoring the back-reaction of the gravitational waves into the fluid dynamics [**2012PhRvD..85d4023C**]. However, the application of this constrained scheme and assessment of its performance in modelling

more generic dynamical spacetimes without symmetry is still a largely unexplored area.

It is worth to point out that the fully constrained scheme of Bonazzola *et al.* [**2004PhRvD..70j4007B**] automatically reduces to the so-called conformally flat condition (CFC) approximation to general relativity [**wilson˙mathews˙2003**, **2008IJMPD..17..265I**] if a tensor field $h_{ij}$ introduced in their formulation is set to zero (see [**XCFC**] for a detailed discussion). The CFC approximation results in a simpler set of elliptic equations for the metric sector. Numerical simulations based on the CFC scheme have been successfully carried out for various astrophysical problems [**2002A&A...393..523D**, **2002PhRvD..65j3005O**, **2004ApJ...615..866S**, **2012PhRvD..86f3001B**, **2013ApJ...773...78B**, **2014PhRvD..90b3002B**, **2015MNRAS.453** and the scheme has also been shown to be a good approximation to full general relativity in rotating iron core collapses [**2007CQGra..24S.139O**].

We have in our mind a motivation to experiment and develop our own general relativistic hydrodynamics code based on the fully constrained formulation of Bonazzola *et al.* [**2004PhRvD..70j4007B**] (or other similar constrained formulations if available in the future) which maximizes the use of elliptic-type equations for the metric sector of the system in the evolution. In this thesis, we take a first step along this direction by developing a relativistic hydrodynamics code based on the xCFC scheme, an improved version of CFC scheme. Although it is not fully general relativistic, the xCFC scheme contains a set of similar, but simpler, elliptic equations as the fully constrained formulation. We can thus use the xCFC scheme to evaluate the performance and robustness of our metric solver.

In this chapter, we first describe the standard 3+1 formalism in general relativity. Then the essential ingredients to formulate a constrained scheme such as conformal decomposition and gauge condition are introduced. Finally, we present a constrained evolution scheme in numerical relativity based on CFC approximation, and the implementation of this scheme.

## 2.2 The $3+1$ decomposition of spacetime

We use the standard ADM (Arnowitt-Deser-Misner) 3+1 formalism [**2007gr.qc.....3035G**, **2008itnr.book.....A**]. In particular, we foliate the four-dimensional spacetime with a set of non-interecting spacelike hypersurfaces (Cauchy surfaces) $\Sigma_t$, which are parametrized by a global time function $t$. We denote the future-pointing, timelike unit vector field which is normal to the hypersurfaces $\Sigma_t$ as $n^\mu$, i.e., $n^\mu$ is normal to the hypersurface $\Sigma_t$ at each point ($n_\mu \propto \nabla_\mu t$) and satisfies $n^\mu n_\mu = -1$. The induced spatial metric $\gamma_{\mu\nu}$ on each hypersurface in the spacetime $g_{\mu\nu}$ can then be expressed as

$$\gamma_{\mu\nu} \equiv g_{\mu\nu} + n_\mu n_\nu, \tag{2.1}$$

where $n^\mu \gamma_{\mu\nu} = 0$. Note that $\gamma^\mu_{\ \nu}$ can be used as a projection operator which maps a spacetime tensor to a spatial tensor on a spatial hypersurface.

Let $t^\mu$ be a timelike vector field on the spacetime which is the tangent to the fime axis, $t^\mu = (\partial/\partial t)^\mu$, and $t^\mu \nabla_\mu t = t^t = 1$. Since $t^\mu$ is not always normal to $\Sigma_t$ (in general, it has components both on $\Sigma_t$ and along $n^\mu$), we further express $t^\mu = \alpha n^\mu + \beta^\mu$ by decomposing it into two components as

$$\alpha \equiv -t^\mu n_\mu, \qquad \beta^\nu \equiv t^\mu \gamma_\mu^{\ \nu}. \tag{2.2}$$

Here, $\alpha$ is called the lapse function, which indicates the rate of advance of time along a timelike unit vector $n^\mu$ normal to a hypersurface while $\beta^i$ is the spacelike shift vector which states the motion of the coordinates within a surface. Note that $n_\mu$ can be expressed as $n_\mu = -\alpha \nabla_\mu t$.

It is convince to express the normal vector $n^\mu$ and $n_\mu$ in terms of $\alpha$ and $\beta^i$, namely,

$$n^\mu = \left(1/\alpha, \beta^i/\alpha\right), \qquad n_\mu = \left(-\alpha, \vec{0}\right). \tag{2.3}$$

The four-dimensional line element can then be written as

$$\begin{aligned} ds^2 &= g_{\mu\nu} dx^\mu dx^\nu \\ &= -\alpha^2 dt^2 + \gamma_{ij}\left(dx^i + \beta^i dt\right)\left(dx^j + \beta^j dt\right), \end{aligned} \tag{2.4}$$

and the spacetime metric as

$$g_{\mu\nu} = \begin{pmatrix} -\alpha^2 + \beta^k\beta_k & \beta_j \\ \beta_i & \gamma_{ij} \end{pmatrix}, \qquad g^{\mu\nu} = \begin{pmatrix} -1/\alpha^2 & \beta^j/\alpha^2 \\ \beta^i/\alpha^2 & \gamma^{ij} - \beta^i\beta^k/\alpha^2 \end{pmatrix}. \tag{2.5}$$

It is can be seen from equation(2.5) that

$$\sqrt{-g} = \alpha\sqrt{\gamma}, \tag{2.6}$$

where $g$ is the determinant of $g_{\mu\nu}$ while $\gamma$ is the determinant of $\gamma_{ij}$.

The energy-momentum tensor $T^{\mu\nu}$ can be decomposit as

$$T_{\mu\nu} = U n_\mu n_\nu + S_\mu n_\nu + S_\nu n_\mu + S_{\mu\nu}, \tag{2.7}$$

where

$$U \equiv n^\mu n^\nu T_{\mu\nu}, \tag{2.8}$$

$$S_\mu \equiv -\gamma^\alpha_{\ \mu} n^\beta T_{\alpha\beta}, \tag{2.9}$$

$$S_{\mu\nu} \equiv \gamma^\alpha_{\ \mu}\gamma^\beta_{\ \nu} T_{\alpha\beta}. \tag{2.10}$$

In the 3+1 formalism, the Einstein equations are split into a set of constraint equations which must be satisfied on every hypersurface

$$R + K^2 - K_{ij}K^{ij} = 16\pi U, \qquad \text{(Hamiltonian constraint)} \tag{2.11}$$

$$\nabla_i(K^{ij} - \gamma^{ij}K) = 8\pi S^i, \qquad \text{(momentum constraint)} \tag{2.12}$$

and a set of the evolution equations for $\gamma_{ij}$ and the extrinsic curvature $K_{ij}$

$$\partial_t \gamma_{ij} = -2\alpha K_{ij} + \nabla_i\beta_j + \nabla_j\beta_i, \qquad \text{(three-metric evolution)} \tag{2.13}$$

$$\begin{aligned} \partial_t K_{ij} = &-\nabla_i\nabla_j\alpha + \alpha\left(R_{ij} + KK_{ij} - 2K_{ik}K^k_{\ j}\right) \\ &+ \beta^k\nabla_k K_{ij} + K_{ik}\nabla_j\beta^k + K_{jk}\nabla_i\beta^k \\ &- 4\pi\alpha\left[2S_{ij} - \gamma_{ij}\left(S^k_{\ k} - U\right)\right], \end{aligned} \qquad \text{(extrinsic curvature evolution)} \tag{2.14}$$

where $\nabla_i$ is the covariant derivative with respect to the three-metric $\gamma_{ij}$, $R_{ij}$ is the corresponding Ricci tensor, $R$ is the scalar curvature and $K$ is the trace of the extrinsic curvature $K_{ij}$.

### 2.2.1 The ADM formulation

## 2.3 Conformal decomposition

### 2.3.1 Conformal decomposition of the 3-metric

In the conformal decomposition formulation, with a time independent flat background metric $f_{ij}$ an appropriately-chosen conformal factor $\psi$, we define the *conformal metric* as

$$\tilde{\gamma}_{ij} \equiv \psi^{-4}\gamma_{ij}, \tag{2.15}$$

where

$$\psi \equiv (\gamma/f)^{-12}, \gamma \equiv \det(\gamma_{ij}), f \equiv \det(f_{ij}). \tag{2.16}$$

Note that, by construction, the conformal metric satisfies

$$\det(\tilde{\gamma}_{ij}) = f. \tag{2.17}$$

The *inverse conformal metric* $\tilde{\gamma}^{ij}$ is defined by

$$\tilde{\gamma}^{ij} \equiv \psi^4\gamma^{ij}. \tag{2.18}$$

### 2.3.2 Conformal decomposition of the Extrinsic Curvature

Firstly, we decompose the extrinsic curvature $K$ of the hypersurface $\Sigma_t$ into trace and traceless parts, namely,

$$A_{ij} \equiv K_{ij} - \frac{1}{3}\gamma_{ij}K, \qquad K \equiv \gamma^{ij}K_{ij}, \tag{2.19}$$

so that $A_{ij}$ is by construction traceless, i.e. $\gamma^{ij}A_{ij} = 0$. Therefore, the traceless decomposition of $K$ are:

$$K_{ij} = A_{ij} + \frac{1}{3}\gamma_{ij}K, \qquad K^{ij} = A^{ij} + \frac{1}{3}\gamma^{ij}K. \tag{2.20}$$

We can then perform the conformal decomposition of the traceless part of $K$ by expressing

$$A_{ij} \equiv \psi^a\tilde{A}_{ij} \tag{2.21}$$

with some power $a$. There are two natural choices of $a$.

**"Time-evolution" scaling:** $a = -4$

One is the "time-evolution" scaling: $a = -4$, which is suggested by the three-metric evolution equation (2.13), was originally introduced by Nakamura in 1994 [**1994reco.conf..155N**]. With this scaling, we define

$$A_{ij} \equiv \psi^{-4}\tilde{A}_{ij}. \tag{2.22}$$

Note that indices of the quantities with tilde such as $\tilde{A}_{ij}$ nd $\tilde{A}^{ij}$ are handled by the conformal spatial metric $\tilde{\gamma}_{ij}$. Notice that $\tilde{A}_{ij}$ is traceless:

$$\tilde{A}_{ij}\tilde{\gamma}^{ij} = 0, \tag{2.23}$$

and thus

$$\tilde{A}^{ij} = \psi^4 A^{ij}. \tag{2.24}$$

The Hamiltonian and momentum constrant equations (2.11) and (2.12) can then be expressed as

$$\tilde{\nabla}^2\psi = \frac{1}{8}\psi\tilde{R} - \left[2\pi U + \frac{1}{8}\left(\tilde{A}_{ij}\tilde{A}^{ij} - \frac{2}{3}K^2\right)\right]\psi^5, \tag{2.25}$$

$$\psi^{-6}\tilde{\nabla}_i\left(\psi^6\tilde{A}^i{}_j\right) - \frac{2}{3}\tilde{\nabla}_j K = 8\pi S_j. \tag{2.26}$$

**"Momentum-costraint" scaling:** $a = -10$

Another possible choice is the "momentum-costraint" scaling: $a = -10$, which is suggested by the momentum constraint equation (2.12), was first considered by Lichnerowicz in 1944 [**zbMATH03098911**]. With this scaling, we define

$$\hat{A}^{ij} \equiv \psi^{10} A^{ij}, \tag{2.27}$$

and thus

$$\hat{A}_{ij} = \psi^2 A_{ij}, \tag{2.28}$$

Here we note that, instead of using tilde, we use hat to distinguish the conformal traceless part of extrinsic curvature in this "momentum-constraint" scaling from the case in "time-evolution" scaling. By relating $\tilde{A}_{ij}$ and $\hat{A}_{ij}$

$$\hat{A}_{ij} = \psi^6\tilde{A}_{ij}, \qquad \hat{A}_{ij} = \psi^6\tilde{A}_{ij}, \qquad \text{and} \qquad \hat{A}_{ij}\hat{A}^{ij} = \psi^{12}\tilde{A}_{ij}\tilde{A}^{ij}, \tag{2.29}$$

the Hamiltonian and momentum constrant equations (2.25) and (2.26) become

$$\tilde{\nabla}^2\psi = \frac{1}{8}\psi\tilde{R} - \left[2\pi U - \frac{1}{12}K^2\right]\psi^5 - \frac{1}{8}\hat{A}_{ij}\hat{A}^{ij}\psi^{-7}, \tag{2.30}$$

$$\tilde{\nabla}_j\hat{A}^{ij} - \frac{2}{3}\psi^6\tilde{\nabla}^i K = 8\pi\psi^{10}S^i. \tag{2.31}$$

Equation (2.30) is the *Lichnerowicz equation*. Note that equations (2.25) and (2.30) are non-linear elliptic equations for $\psi$. Although equations (2.25) and (2.30) are technically the same equations, the mathematical properties of them are significantly different if we treat them as non-linear elliptic equations for $\psi$. For example, the power of $\psi$ in the quadratic extrinsic curvature $A^2$ term (i.e. the positive power $(+5)$ in equation (2.25) and the negative power $(-7)$ in equation (2.30)) affects the local uniqueness of the solutions [**1979sgrr.work...83Y**, **evans1998partial**, **XCFC**].

## 2.4 Maximal slicing

Maximal slicing, a gauge condition which corresponds to the vanishing of the mean curvature of the hypersurfaces, is defined by

$$K = 0 = \partial_t K. \tag{2.32}$$

Not only the maximal slicing has a clear geometrical meaning, it can be treated as an natural extention of Newtonian gravity and it has a singularity-avoidance property.

**Natural Newtonian limit**

The Maximal slicing can be considered as a natural generalization to the relativistic case of the canonical slicing of Newtonian spacetime by hypersurfaces of constant absolute time. From equation (2.14), it can be shown that

$$\nabla_i \nabla^i \alpha = \alpha \left[ 4\pi \left( S^k_k + U \right) + A_{ij} A^{ij} \right], \tag{2.33}$$

where $A_{ij}$ is the tracefree part of $K_{ij}$. Now, let's consider the Newtonian limit of equation (2.33). Assuming the gravitational field is weak and static, we have:

$$\alpha \approx 1 + \Phi, \qquad \gamma_{ij} \approx (1 + 2\Phi) f_{ij}, \qquad K_{ij} = 0, \qquad |\Phi| \ll 1, \tag{2.34}$$

where $\Phi$ is the Newtonian gravitational potential. In addition, the matter is assumed to be non-relativistic, i.e.,$|S^i_j| \ll U$, which implies $U \approx \rho_0$, where $\rho_0$ is the proper reset-mass energy density. As a result, at the Newtonian limit, equation (2.33) reduces to the Poisson equation for the gravitational potential

$$\nabla_i \nabla^i \Phi = 4\pi \rho_0. \tag{2.35}$$

**Singularity-avoidance**

Another nice property of the maximal slicing is singularity-avoidance. Since $K = 0$ is equivalent to $\nabla_\nu n^\nu = 0$ (incompressibility condition), which implies that only timelike unit normal vector field is considered, the apperance of an irregular region on spatial hypersurfaces is prohibited.

The singularity-avoidance property under this gauge condition can be found from equation (2.13), yields

$$\partial_t \sqrt{\gamma} = \partial_i \left( \sqrt{\gamma} \beta^i \right). \tag{2.36}$$

This equation shows that under maximal slicing, the proper volume element $\sqrt{\gamma}$ satisfies a continuity equation and is likely to have a singularity-avoidance property. Therefore, as far as a regular shift vector $\beta^i$ is chosen and initial condition for $\gamma_{ij}$ is regular, $\gamma$ is regular forever.

This singularity-avoidance property can also be seen from another point of view. By combining the Hamiltonian constraint equation (2.25), equation (2.33) can be expressed as

$$\tilde{\nabla}^2 (\alpha\psi) = (\alpha\psi) \left[ \frac{1}{8} \tilde{R} + 2\pi \left( U + 2S \right) \psi^4 + \frac{7}{8} \tilde{A}_{ij} \tilde{A}^{ij} \psi^4 \right]. \tag{2.37}$$

Equations (2.33) and (2.37) suggest that $\alpha$ and $\alpha\psi$ should be smooth functions as far as the spatial metric is regular since they are solutions of these elliptic equations.

## 2.5 Toward Constrained Schemes for the Einstein field equations

While the standard $3 + 1$ formulation introduced in section 2.2 is a well-defined initial-value formulation in general relativity, it is difficult to maintain the constraint equations in the numerical evolution of the evolution equations above because the

ADM equations (2.11)-(2.14) are numerically unstable. There are serveral different re-formulations of $3+1$ numerical relativity that can lead to stable evolutions [**1995PhRvD..52.5428S**, **1999PhRvD..59b4007B**, **2003PhRvD..67j4005B**, **2010PhRvD..81h4003B**]. However, these schemes are based on a free-evolution approach where the Einstein equations are evolved with hyperbolic-type equations. The constraint equations are only used for solving the initial data and serve as a monitor for numerical errors during the simulations.

We have a motivation to develop efficient solvers for elliptic-type metric equations that one needs in order to carry out fully-constrained evolutions for numerical relativity. As a first step towards this goal, our relativistic hydrodynamics code `Gmunu` employs the Isenberg-Wilson-Mathews (also known as conformal flatness condition) approximation to general relativity. In this section, we describe the formulation based on conformal flatness condition approximation and the implementation of this constrained scheme.

### 2.5.1 Isenberg-Wilson-Mathews Approximation to General Relativity (Conformal Flatness condition)

A (gravitational-)waveless approximation to general relativity was originally proposed by Isenberg in 1978 (the work was published thirty-years later [**2008IJMPD..17..265I**]), and has been reintroduced indepently by Wilson and Mathews in 1989 [**1989fnr..book..306W**]. This approximation is now named as Isenberg-Wilson-Mathews (IWM) approximation, or the conformal flatness condition (CFC).

In the CFC approximation [**CoCoA**, **XECHO**], the three metric $\gamma_{ij}$ is assumed to be decomposed according to

$$\gamma_{ij} \equiv \psi^4 f_{ij}, \qquad \text{(conformally flat)} \tag{2.38}$$

where $f_{ij}$ is a time independent flat background metric and $\psi$ is the conformal factor which is a function of space and time. With maximal slicing conditions (2.32), one can derive the time derivative of the conformal factor $\psi$ and also the extrinsic curvature $K_{ij}$

$$\partial_t \psi = \frac{\psi}{6} \nabla_k \beta^k, \tag{2.39}$$

$$K_{ij} = \frac{1}{2\alpha} \left( \nabla_i \beta_j + \nabla_j \beta_i - \frac{2}{3} \gamma_{ij} \nabla_k \beta^k \right). \tag{2.40}$$

The CFC approximation of the ADM equations can be reduced into three coupled non-linear elliptic equations (two scalar equations and one vector equation) for the three unknowns $\alpha$, $\psi$ and $\beta^i$:

$$\tilde{\Delta}\psi = \left( -2\pi U - \frac{1}{8} K^{ij} K_{ij} \right) \psi^5, \tag{2.41}$$

$$\tilde{\Delta}(\alpha\psi) = \alpha\psi^5 \left[ 2\pi \left( U + 2S \right) + \frac{7}{8} K_{ij} K^{ij} \right], \tag{2.42}$$

$$\tilde{\Delta}\beta^i + \frac{1}{3} \tilde{\nabla}^i \left( \tilde{\nabla}_j \beta^j \right) = 16\pi\alpha\psi^4 f^{ij} S_i + 2\psi^{10} K^{ij} \tilde{\nabla}_j \left( \alpha\psi^{-6} \right), \tag{2.43}$$

where $\tilde{\nabla}_i$ and $\tilde{\Delta} \equiv \tilde{\nabla}_i \tilde{\nabla}^i$ are the covariant derivative and the Laplacian with respect to the flat three metric $f_{ij}$, respectively.

Note that the CFC approximation is exact for spherically symmetric spacetimes and is correct at the 1-PN order in the post-Newtonian expansion of general relativity. Numerical simulations based on the CFC scheme have been successfully carried out for various astrophysical problems [**2002A&A...393..523D**, **2002PhRvD..65j3005O**, **2004ApJ...615..866S**, **2006MNRAS.368.1609D**, **2012PhRvD..86**
**2013ApJ...773...78B**, **2014PhRvD..90b3002B**, **2015MNRAS.453..287M**] and the scheme has also been shown to be a good approximation to full general relativity in axisymmetric rotating neutron stars [**1996PhRvD..53.5533C**, **2002A&A...393..523D**, **2006MNRAS.368.1609D**] and in rotating iron core collapses [**2007CQGra..24S.139O**].

### 2.5.2 Extended CFC Scheme

While the CFC scheme disbribed in above subsection 2.5.1 (i.e. solving the metric equations (2.41)-(2.43)) have been successfully applied in various astrophysical problems, this scheme suffers from mathematical non-uniqueness problems when the system is highly relativistic. In order to overcome the non-uniqueness issue, the scheme was reformulated and extended to the so-called extended CFC (xCFC) scheme so that the modelling of extreme spactimes such as black hole formation becomes possible [**XCFC**, **2019MNRAS.484.3307M**, **2012PhRvD..85d4023C**]. In the xCFC scheme, one introduces a vector field $X^i$, and the metric can be solved by the following equations:

$$\tilde{\Delta} X^i + \frac{1}{3}\tilde{\nabla}^i\left(\tilde{\nabla}_j X^j\right) = 8\pi f^{ij}\tilde{S}_j, \tag{2.44}$$

$$\tilde{\Delta}\psi = -2\pi\tilde{U}\psi^{-1} - \frac{1}{8}f_{ik}f_{jl}\tilde{A}^{kl}\tilde{A}^{ij}\psi^{-7}, \tag{2.45}$$

$$\tilde{\Delta}(\alpha\psi) = (\alpha\psi)\left[2\pi\left(\tilde{U}+2\tilde{S}\right)\psi^{-2} + \frac{7}{8}f_{ik}f_{jl}\tilde{A}^{kl}\tilde{A}^{ij}\psi^{-8}\right], \tag{2.46}$$

$$\tilde{\Delta}\beta^i + \frac{1}{3}\tilde{\nabla}^i\left(\tilde{\nabla}_j\beta^j\right) = 16\pi\alpha\psi^{-6}f^{ij}\tilde{S}_i + 2\tilde{A}^{ij}\tilde{\nabla}_j\left(\alpha\psi^{-6}\right), \tag{2.47}$$

where $\tilde{\nabla}_i$ and $\tilde{\Delta}$ are the covariant derivative and the Laplacian with respect to the flat three metric $f_{ij}$, respectively, and $\tilde{U} \equiv \psi^6 U$, $\tilde{S}_i \equiv \psi^6 S_i$ and $\tilde{S} \equiv \psi^6 S = \psi^6\gamma_{ij}S^{ij}$ are the rescaled matter source terms. The conformal decomposition of the traceless part of $K$, $\tilde{A}^{ij}$, can be approximated on the CFC approximation level by (see the Appendix of [**XCFC**]):

$$\tilde{A}^{ij} \approx \tilde{\nabla}^i X^j + \tilde{\nabla}^j X^i - \frac{2}{3}\tilde{\nabla}_k X^k f^{ij}. \tag{2.48}$$

#### Metric solver with xCFC scheme

By following [**XCFC**], the metric equations (2.44)-(2.47) can be decoupled, thus they can be solved in a hierarchical way and the local uniqueness is guaranteed. Once the conformally rescaled variables $\tilde{U}$ and $\tilde{S}_i$ (which can be expressed in terms of the conformally rescaled hydrodynamical conserved variables such as $(q_D, q_{S_i}, q_\tau)$, see section fixme) are known, the metric equations can be solved accordingly.

The steps for solving the metric equations are summarized in the following:

Step 1: Solve equation (2.44) for the vector field $X^i$ from the conserved variables $\tilde{S}_i$.

Step 2: Calculate the tensor $\tilde{A}^{ij}$ in equation (2.48) from the vector potential $X^i$.

Step 3: Solve equation (2.45) for the conformal factor $\psi$.

Step 4: With the updated conformal factor $\psi$, $\tilde{S}$ can be worked out consistently[1].

Step 5: Solve equation (2.46) for the lapse function $\alpha$.

Step 6: Solve equation (2.47) for the shift vector $\beta^i$.

Note that due to the non-linearity of the scalar equations (2.45) and (2.46), instead of solving $\psi$ and $\alpha$ directly, we solve for its deviation, e.g. $\delta_\psi \equiv \psi - 1$ as in [**2020CQGra..37n5015C**, **XECHO**]. On the other hand, the Laplacian of a vector field is non-trvial. In our implementation for the vectorial elliptic equations, we solve for the orthonormal-basis components for vector fields instead of coordinate-basis components. Some useful relations for implementating this metric solver in different coordinate can be found in appendix A.

### Boundary conditions

To solve the metric equations, appropriate boundary conditions at the origin and outer computational boundary are required. In the practical simulations of spheric-like astrophysical systems (e.g. isolated neutron star and core-collapse supernova), as the spacetime at the star surface is close to spherically symmetric, setting the Schwarzschild solution as the outer boundary condition is usually a good approximation [**CoCoA**, **CoCoNuT**]. In order to let the solution fall off as the Schwarzschild solution at large distance, we require $\psi = \frac{C}{r} + 1$, $\alpha = \frac{C}{r} + 1$ and $X^i = \beta^i = 0$ at the outer boundary ($r = r_{\rm max}$). In `Gmunu`, we impose the boundary conditions

$$\left.\frac{\partial \psi}{\partial r}\right|_{r_{\rm max}} = \frac{1-\psi}{r}, \qquad \left.\frac{\partial \alpha}{\partial r}\right|_{r_{\rm max}} = \frac{1-\alpha}{r}, \tag{2.49}$$

$$\left.\beta^i\right|_{r_{\rm max}} = 0, \qquad \left.X^i\right|_{r_{\rm max}} = 0. \tag{2.50}$$

The boundary conditions (2.49) we implemented in `Gmunu` for the equation of the conformal factor $\psi$ is

$$\frac{\partial}{\partial r}\left(r\delta_\psi\right) = 0. \tag{2.51}$$

In spherical coordinate $(r, \theta, \phi)$, the implementation of this Robin boundary condition (2.51) on the cell-face is straightforward. However, this is not the case when we are working on cartesian coordinate $(x, y, z)$ or cylindrical coordinate $(R, z, \varphi)$. In these particular cases, we define the outer boundary at the outer most cell-center, the boundary condition (2.51) can then be implmenetated as

$$\begin{cases} \delta_\psi + x\frac{\partial \delta_\psi}{\partial x} + y\frac{\partial \delta_\psi}{\partial y} + z\frac{\partial \delta_\psi}{\partial z} = 0 & \text{in cartesian coordinate } (x, y, z), \\ \delta_\psi + R\frac{\partial \delta_\psi}{\partial R} + z\frac{\partial \delta_\psi}{\partial z} = 0 & \text{in cylindrical coordinate } (R, z, \varphi). \end{cases} \tag{2.52}$$

[1]When the metric solver is coupled with a hydrodynamics code, $\tilde{S}$ can be worked out by calculating the conserved variables $(D, S_i, \tau)$ based on the updated $\psi$ and thus convert the conserved variables to the primitive variables $(\rho, Wv^i, P)$. The definition of conserved variables and primitive variables can be found in section fixme

# Chapter 3

# Formulations of the Relativistic Hydrodynamical Equations

In chapter 2, we discussed mostly the left-hand side of the Einstein equation, and the formulation we adopted in `Gmunu`. In this chapter, we focus on the right-hand side of the Einstein equation, i.e., the $3+1$ treatment of non-gravitational field such as matter or eletromagnetic field.

## 3.1 The $3+1$ "Valencia" Formulation

In this section, we consider the *perfect fluid* without dissipation (i.e., no viscosity and heat fluxes). The energy-momentum tensor of the perfect fluid can be expressed as

$$T^{\mu\nu}_{\rm fluid} = \rho h u^\mu u^\nu + p g^{\mu\nu}, \tag{3.1}$$

where $\rho$ is the rest-mass density of the fluid, $u^\mu$ is the fluid four-velocity, $p$ is the pressure, $h = 1+\epsilon+p/\rho$ is the specific enthalpy, and $\epsilon$ is the specific internal energy.

The *Lorentz factor* of the fluid with respect to the Eulerian observer is defined as the proportional factor $W$ between the proper times $d\tau_0$ and $d\tau$, namely, $d\tau \equiv W d\tau_0$, and hence the lorentz facfor $W$ can be obtained by contracting the fluid's 4-velocities and the Eulerian obvserver's 4-velocities

$$W = -n_\mu u^\mu = \alpha u^t. \tag{3.2}$$

The the 3-velocity seen by an Eulerian obvserver at rest in current spatial 3-hypersurface can be expressed as $v^i = u^i/W + \beta^i/\alpha$. As a result, the Lorentz factor satisifies $W = 1/\sqrt{1-v^i v_i}$.

### Rest-mass Conservation

The rest-mass density $\rho$ obeys the rest-mass conservation equation, or the so-called continuity equation

$$\nabla_\mu \left(\rho u^\mu\right) = 0. \tag{3.3}$$

With some calculation, this equations can be expressed as

$$\partial_t \left(\sqrt{\gamma} D\right) + \partial_i \left[\sqrt{\gamma} D \left(\alpha v^i - \beta^i\right)\right] = 0, \tag{3.4}$$

where $D \equiv \rho W$, is the conserved density.

## Energy and Momentum Conservation

In addition to conservation of rest-mass (3.3), the conservation of the energy-momentum must also be satisfied. In particular, the conservation of energy-momentum is

$$\nabla_\mu T^\mu_{\ \nu} = 0, \tag{3.5}$$

where $T^{\mu\nu}$ is the total energy-momentum tensor. Recall that in the 3+1 formulation, the energy-momentum tensor $T^{\mu\nu}$ can be decomposed as (2.7),

$$T_{\mu\nu} = U n_\mu n_\nu + S_\mu n_\nu + S_\nu n_\mu + S_{\mu\nu}, \tag{3.6}$$

where

$$U \equiv n^\mu n^\nu T_{\mu\nu}, \tag{3.7}$$
$$S_\mu \equiv -\gamma^\alpha_{\ \mu} n^\beta T_{\alpha\beta}, \tag{3.8}$$
$$S_{\mu\nu} \equiv \gamma^\alpha_{\ \mu}\gamma^\beta_{\ \nu} T_{\alpha\beta}. \tag{3.9}$$

The Euler and energy equations can be obtained by projecting the conservation equation of energy-momentum tensor to the normal vector $n^\mu$ and into the spatial hypersurface $\Sigma_t$, namely

$$\gamma_i^{\ \nu}\nabla_\mu T^\mu_{\ \nu} = 0, \qquad \text{(Euler equation)} \tag{3.10}$$
$$n^\nu \nabla_\mu T^\mu_{\ \nu} = 0. \qquad \text{(Energy equation)} \tag{3.11}$$

After some calculations, we have

$$\partial_t\left(\sqrt{\gamma}S_j\right) + \partial_i\left[\sqrt{\gamma}\left(\alpha S^i_{\ j} - \beta^i S_j\right)\right] = \sqrt{\gamma}\left(\frac{1}{2}\alpha S^{ik}\partial_j\gamma_{ik} + S_i\partial_j\beta^i - U\partial_j\alpha\right), \tag{3.12}$$
$$\partial_t\left(\sqrt{\gamma}U\right) + \partial_i\left[\sqrt{\gamma}\left(\alpha S^i - \beta^i U\right)\right] = \sqrt{\gamma}\left(\alpha S^{ik}K_{ik} - S^i\partial_i\alpha\right). \tag{3.13}$$

## Conservative form of hydrodynamics equations

For perfect fluid, since the energy-momentum tensor is given by equation (3.1), the $3+1$ component of the energy-momentum tensor can be expressed as

$$U = \rho h W^2 - p, \tag{3.14}$$
$$S_\mu = \rho h W^2 v_\mu, \tag{3.15}$$
$$S_{\mu\nu} = \rho h W^2 v_\mu v_\nu + p\gamma_{\mu\nu}. \tag{3.16}$$

Also, since linear combinations of conserved variables are still solutions of the equations in conservative form, it is possible to introduce another form of conserved energy

$$\tau \equiv U - D = \rho W\left(hW - 1\right) - p, \tag{3.17}$$

thus the energy equation (3.13) can be written as

$$\partial_t\left(\sqrt{\gamma}\tau\right) + \partial_i\left[\sqrt{\gamma}\left(\alpha\left(S^i - Dv^i\right) - \beta^i\tau\right)\right] = \sqrt{\gamma}\left(\alpha S^{ik}K_{ik} - S^i\partial_i\alpha\right). \tag{3.18}$$

Form numerical point of view, the conservation of $\tau$ as a combination of two conserved quantities is more accurate than solving $U$ only.

By collecting equations (3.4), (3.12) and (3.18), the relativistic-hydrodynamic equations can be expressed ad the conservative form

$$\partial_t \left(\sqrt{\gamma}\boldsymbol{Q}\right) + \partial_i \left(\sqrt{\gamma}\boldsymbol{F}^i\right) = \sqrt{\gamma}\boldsymbol{S}, \tag{3.19}$$

where

$$\boldsymbol{Q} = \begin{bmatrix} D \\ S_j \\ \tau \end{bmatrix} = \begin{bmatrix} \rho W \\ \rho h W^2 v_j \\ \rho h W^2 - p - D \end{bmatrix}, \tag{3.20}$$

$$\boldsymbol{F^i} = \begin{bmatrix} D\left(\alpha v^i - \beta^i\right) \\ S_j\left(\alpha v^i - \beta^i\right) + \alpha \delta^i_j p \\ \tau\left(\alpha v^i - \beta^i\right) + \alpha p v^i \end{bmatrix}, \tag{3.21}$$

$$\boldsymbol{S} = \begin{bmatrix} 0 \\ \frac{1}{2}\alpha S^{ik}\partial_j \gamma_{ik} + S_i \partial_j \beta^i - U \partial_j \alpha \\ \alpha S^{ik} K_{ik} - S^i \partial_i \alpha \end{bmatrix}. \tag{3.22}$$

## 3.2 The reference-metric formulation

## 3.3 Conserved to Primitive variables conversion

## 3.4 Radiation hydrodynamics

### 3.4.1 Boltzmann's equation

### 3.4.2 Moment formalism

# Chapter 4

# Numerical methods

## 4.1 Numerical methods for hydrodynamics

### 4.1.1 Finite volume methods

#### 4.1.1.1 Godunov's Method

#### 4.1.1.2 Total-Variation-Diminishing Schemes

#### 4.1.1.3 Reconstruction Schemes

#### 4.1.1.4 Riemann solvers

#### 4.1.1.5 High-Order Finite volume methods

### 4.1.2 Finite difference methods

#### 4.1.2.1 Lax-Friedrichs Flux Splitting

### 4.1.3 Time Discretization

#### 4.1.3.1 Strong Stability-Preserving Runge-Kutta Methods

#### 4.1.3.2 Courant-Friedrichs-Lewy Condition

#### 4.1.3.3 Implicit-explicit Schemes

### 4.1.4 Atmosphere Treatment

#### 4.1.4.1 Positivity Preserving Limiter

## 4.2 Multigrid methods for elliptic equations

### 4.2.1 An overview of multigrid

Multigrid is an efficient method for solving elliptic partial differential equations with low memory and work complexity. Different modes are filtered out with different rates at different resolutions. For some low-frequency modes, it is computationally expensive to compute directly on a high-resolution discretization. However, it can be done efficiently at a low-resolution discretization. The main concept of the multigrid method is to solve the problem recursively with a series of coarse grids. It is noted that the multigrid method is not a single method but a strategy with many possible

implementations. However, the elements needed to construct a multigrid solver is more or less the same for different implementations. For instance, as shown in figure 4.1, the key ingredients of multigrid solver includes (1) a *cycle framework*, the backbone of the whole solver which describe the structure of the multigrid solver (see figure 4.1 for examples), (2) inter grid transfer operators to connect the solver with different levels, where the operators that map the values from a fine to a coarse grid are called *restriction* and the mapping from a coarse to the fine grid are called *prolongation*. (3) *smoothers* to smooth the solutions at different resolutions and (4) *direct solvers* to obtain the solutions at the coarsest level.

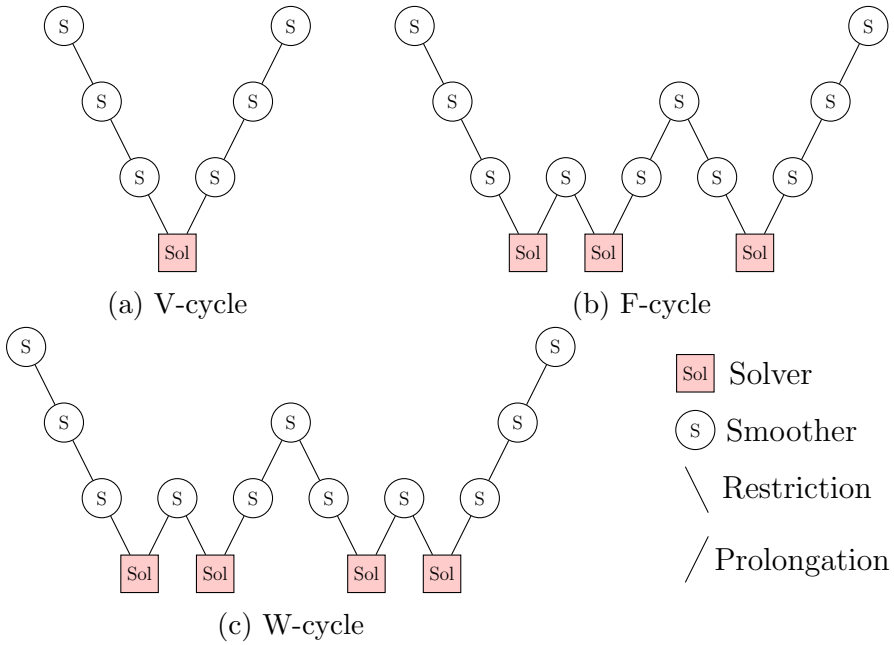


(a) V-cycle (b) F-cycle (c) W-cycle

Figure 4.1: Three types of (4-grid) cycles can be used in multigrid methods. "S" denotes smoothing while "Sol" denotes solving the equation directly. Each descending line \ represents restriction and each ascending line / represents prolongation. The key ingredients of multigrid solver includes a cycle framework, restriction and prolongation operators, smoothers and solvers.

### 4.2.2 Nonlinear multigrid: The Full Approximation Scheme

Due to the nonlinearity of the Einstein equations needed to be solved (i.e. Eqs. (2.44)-(2.47)), nonlinear multigrid method is required. The implementations for the multigrid for non-linear elliptic equations are different from the linear cases. Two well-known methods for solving non-linear partial differential equations with multigrid techniques are the Full Approximation Scheme (FAS) [**MR431719**] and Newton-multigrid (Newton-MG) [**briggs2000multigrid**, **trottenberg2001multigrid**]. The two methods are widely used and obtained successes in various problems. We refer the interested reader to [**BRABAZON20141619**] for a detailed comparison of the two methods. Due to the fact that the memory used is low in FAS, the current version of `Gmunu` adopts the FAS algorithm (see [**MR431719**, **BRABAZON20141619**, **press1996numerical**] and references therein for more details).

Here we briefly outline how the Full Approximation Scheme works. To solve an nonlinear elliptic equation $\mathcal{L}(u) = f$, where $\mathcal{L}$ is some elliptic operator, $u$ is the

solution and $f$ is the source term, we can discretize the equation on a grid with resolution $h$ as

$$\mathcal{L}_h(u_h) = f_h. \tag{4.1}$$

Suppose we have obtained an approximate solution $\tilde{u}_h$ through the smoothing processes (note that smoothers is a kind of solver, but slow), we can find the desired correction $e_h$ so that the equation $\mathcal{L}_h(\tilde{u}_h + e_h) = f_h$ is solved. The residual $r_h$ is defined by

$$\begin{aligned} r_h :=& \mathcal{L}_h(\tilde{u}_h + e_h) - \mathcal{L}_h(\tilde{u}_h) \\ =& f_h - \mathcal{L}_h(\tilde{u}_h) \end{aligned} \tag{4.2}$$

By transfering the first line of the Eq. (4.2) to a coarse grid with resolution $2h$ through the restriction operator $\mathcal{R}$, we have

$$\mathcal{L}_{2h}(u_{2h}) = \mathcal{R}(u_h) - \mathcal{L}_{2h}(\mathcal{R}(\tilde{u}_h)). \tag{4.3}$$

Note that the RHS of Eq. (4.3) can now be treated as a new source term, that is, $f_{2h} := \mathcal{R}(u_h) - \mathcal{L}_{2h}(\mathcal{R}(\tilde{u}_h))$. Let $v$ denote the approximate solution of Eq. (4.3), we can then obtain the coarse-grid correction:

$$\tilde{e}_{2h} = v - \mathcal{R}(u_h), \tag{4.4}$$

and thus the new approximate solution on resolution $h$ is

$$\begin{aligned} \tilde{u}_h^{\text{new}} =& \tilde{u}_h + \mathcal{P}(\tilde{e}_{2h}) \\ =& \tilde{u}_h + \mathcal{P}(v - \mathcal{R}(u_h)), \end{aligned} \tag{4.5}$$

where $\mathcal{P}$ is the prolongation operator. Note that FAS can also be used to solve linear elliptic equations. Algorithm 1 shows the pseudocode of a single cycle of the non-linear multigrid elliptic partial differential equation solver implemented in

Gmunu.

**Algorithm 1:** A single cycle of the non-linear multigrid elliptic partial differential equation solver implemented in Gmunu.

```
/* Before solving any equations, we have to initialize the γ
   based on what cycle type we want to use.  In particular:   */
/* V-cycle:  set γ = 1                                        */
/* W-cycle:  set γ = 2                                        */
/* F-cycle:  set γ = 2                                        */
/*                                                            */
MG(u_l, f_l)
if l = 1 then
    u_l ← Solve(u_l)
    if F-cycle then
        γ ← 1
    end
else
    u_l ← Smoothing(u_l, f_l) ;                  /* Pre-smoothing */
    r_l ← f_l − L_l(u_l) ;                 /* calculating the residual */
    r_{l−1} ← Restriction(r_l) ;       /* restriction of the residual */
    u_{l−1} ← Restriction(u_l) ;       /* restriction of the solution */
    f_{l−1} ← r_{l−1} + L_{l−1}(u_{l−1}) ;
    v ← u_{l−1} ;
    /* Recursive call for the coarse grid correction          */
    for i = 1 to γ do
        v ← MG(v, f_{l−1})
    end
    u_l ← u_l + Prolongation(v − u_{l−1}) ;        /* Prolongation  */
    u_l ← Smoothing(u_l, f_l) ;                  /* Post-smoothing  */
    if finest level and F-cycle then
        γ ← 2
    end
end
```

### 4.2.3 Cell-centered discretization and intergrid transfer operators

As mentioned in **??**, the source terms of the metric equations consist of the hydrodynamical variables. Meanwhile, since Gmunu solves the hydrodynamics with finite volume approach, the grids are discretized with cell-centred discretization. On the other hand, the discretization for the metric solver is in general different from the hydrodynamics sector. For instance, for the pseudospectral method, the choice of grid points has to be consistent with the basis functions which can not be chosen arbitrarily. The corresponding interpolation or extrapolation are needed so that the hydrodynamical variables can be passed correctly into the metric solver (e.g. [**CoCoNuT**, **XECHO**]), which might be another bottleneck of the computational time of the simulations. In order to adapt the grid of the hydrodynamics sector so that the hydrodynamical variables can be passed into the metric solver without any interpolation or extrapolation, we implemented the cell-centred multigrid (CCMG)

$$\frac{1}{4}\begin{bmatrix} 1 & & 1 \\ & * & \\ 1 & & 1 \end{bmatrix}^{h}_{2h} \qquad \frac{1}{16}\begin{bmatrix} 1 & 3 & & 3 & 1 \\ 3 & 9 & & 9 & 3 \\ & & * & & \\ 3 & 9 & & 9 & 3 \\ 1 & 3 & & 3 & 1 \end{bmatrix}^{h}_{2h}$$

(a) piecewise constant restriction (b) bi-linear prolongation

Figure 4.2: The stencil notation of the interpolation operators implemented in `Gmunu`. The "*" denotes the location of the coarse grid node. The notation shows the weighting of the value which are the neighbors of the coarse grid node "*".

[**Mohr2004**, **MGbook**], which is one of the novelties of `Gmunu`.

Constructing a cell-centred multigrid solver is non-trivial. Unlike the vertex-centred case, in which a node of the coarse grid is also a node of the fine grid, the nodes on coarser grids do not form a subset of the fine grid nodes in the case of cell-centred discretization. The choices of inter-grid transfer operators and the boundary condition implementation are different from the vertex-centred cases. There are also many possible approaches for different situations. Indeed, constructing problem-independent efficient cell-centred transfer operators is still under an active research area in computational physics and applied mathematics (see [**Mohr2004**] and references therein).

There are many possible choices of restriction and prolongation operators and they cannot be chosen arbitrarily [**Mohr2004**, **MGbook**]. In `Gmunu`, we adopt the most standard combination, i.e., piecewise constant restriction (figure 4.2a) and bi-linear prolongation (figure 4.2b).

## Key features of the nonlinear cell-centered multigrid metric solver in `Gmunu`

This section shortly summarizes the key features of the metric solver implemented in `Gmunu`. In our multigrid metric solver, we adopt the Full Approximation Storage (FAS) to deal with the nonlinear metric equations with V-, W- and F-cycle implemented. For the smoother and solvers, we use the standard red-black nonlinear Gauss-Seidel relaxation [**press1996numerical**]. In particular, the smoother consists of 15-times relaxations and the direct solver consists of 200-times relaxations. For the inter-grid transfer operators, we adopt piecewise constant restriction (4.2a) and bi-linear prolongation (4.2b). Note that multigrid solvers are iterative solvers. Practically, this function has to be called until the solution converges, i.e., when the $L_\infty$ or $L_1$ norm of the residual is below some chosen threshold value.

## 4.3 Adaptive Mesh Refinement

### 4.3.1 Overview of AMR

### 4.3.2 refinement cirteria

### 4.3.3 Data structure

# Chapter 5

# Neutron stars

## 5.1 Numerical simulation of NS

### 5.1.1 Overview

### 5.1.2 The Dense Matter EOS of NS

## 5.2 BNS systems

### 5.2.1 The early inspiral

### 5.2.2 The late inspiral and merger

### 5.2.3 Post-merger remnant

### 5.2.4 Quasi-universal relations in BNS simulations

### 5.2.5 The Tidal Effective-One-Body model and Dynamical Tide effects

## 5.3 Asteroseismology of NS

### 5.3.1 Oscillation modes of stars

### 5.3.2 Properties of f-modes

## 5.4 GW asteroseismology with f-modes from NS binaries at the merger phase

### 5.4.1 Numerical setup and initial data

### 5.4.2 Extraction of f-modes

### 5.4.3 Comparing the frequencies of the fundamental oscillation modes to the peak GW amplitude

### 5.4.4 The origin of $Mf_{max}$-$\kappa_2^T$ universal relation

### 5.4.5 Dynamical tide excitation and possible reasonce effects

### 5.4.6 Constraints on EOS and other applications

# Chapter 6

# Core-collapse Supernovae and Neutrino treatments

## 6.1 Numerical simulation of CCSNe

### 6.1.1 Overview

### 6.1.2 Numerical setup and Initial progenitor

### 6.1.3 Collapse dynamics

### 6.1.4 The finite-temperature EOS of CCSNe

#### 6.1.4.1 Tabulated EOS

## 6.2 Numerical simulations of CCSNe including ILEAS neutrino scheme

### 6.2.1 Neutrino interactions in relativistic hydrodynamical equations under CFC approximation

### 6.2.2 The modified neutrino leakage module

#### 6.2.2.1 Reactions for opacities of production rates

#### 6.2.2.2 Reactions for opacities of absorption and optical depth

### 6.2.3 The diffusion time-scale

#### 6.2.3.1 Reactions for opacities of diffusion

### 6.2.4 Neutrino absorption module for optically thin region

### 6.2.5 Neutrino equilibration module for optically thick region

### 6.2.6 Neutrino luminosity and mean energy

### 6.2.7 Astrophysical tests

### 6.2.8 Comparsion to other neutrino schemes

# Chapter 7

# Conclusion

# Appendix A

# Useful relations for implementation in CFC approximation

## A.1 The Extrinsic Curvature $K_{ij}$

The Extrinsic Curvature arise in the gravitational source terms for conserved variable $\tau$, see equation (**??**). Here we explicitly express the extrinsic curvature $K_{ij}$ in different flat background spacetime.

### Cartesian Coordinate

In this case, the line element $ds^2$ can be expressed as

$$ds^2 = \psi^4(dx^2 + dy^2 + dz^2). \tag{A.1}$$

The non-vanishing extrinsic curvature $K_{ij}$ are:

$$K^{xx} = \frac{\gamma^{xx}}{3\alpha}\left(2\frac{\partial\beta^x}{\partial x} - \frac{\partial\beta^y}{\partial y} - \frac{\partial\beta^z}{\partial z}\right), \tag{A.2}$$

$$K^{yy} = \frac{\gamma^{yy}}{3\alpha}\left(-\frac{\partial\beta^x}{\partial x} + 2\frac{\partial\beta^y}{\partial y} - \frac{\partial\beta^z}{\partial z}\right), \tag{A.3}$$

$$K^{zz} = \frac{\gamma^{zz}}{3\alpha}\left(-\frac{\partial\beta^x}{\partial x} - \frac{\partial\beta^y}{\partial y} + 2\frac{\partial\beta^z}{\partial z}\right), \tag{A.4}$$

$$K^{yx} = K^{xy} = \frac{1}{2\alpha}\left(\gamma^{xx}\frac{\partial\beta^y}{\partial x} + \gamma^{yy}\frac{\partial\beta^x}{\partial y}\right), \tag{A.5}$$

$$K^{zy} = K^{yz} = \frac{1}{2\alpha}\left(\gamma^{yy}\frac{\partial\beta^z}{\partial y} + \gamma^{zz}\frac{\partial\beta^y}{\partial z}\right), \tag{A.6}$$

$$K^{xz} = K^{zx} = \frac{1}{2\alpha}\left(\gamma^{zz}\frac{\partial\beta^x}{\partial z} + \gamma^{xx}\frac{\partial\beta^z}{\partial x}\right). \tag{A.7}$$

### Cylindrical Coordinate

In this case, the line element $ds^2$ can be expressed as

$$ds^2 = \psi^4(dR^2 + dz^2 + R^2 d\varphi^2) \tag{A.8}$$

The non-vanishing extrinsic curvature $K_{ij}$ are:

$$K^{RR} = \frac{\gamma^{RR}}{3\alpha}\left(2\frac{\partial\beta^R}{\partial R} - \frac{\partial\beta^z}{\partial z} - \frac{\partial\beta^\varphi}{\partial\varphi} - \frac{\beta^R}{R}\right), \tag{A.9}$$

$$K^{zz} = \frac{\gamma^{zz}}{3\alpha}\left(-\frac{\partial\beta^R}{\partial R} + 2\frac{\partial\beta^z}{\partial z} - \frac{\partial\beta^\varphi}{\partial\varphi} - \frac{\beta^R}{R}\right), \tag{A.10}$$

$$K^{\varphi\varphi} = \frac{\gamma^{\varphi\varphi}}{3\alpha}\left(-\frac{\partial\beta^R}{\partial R} - \frac{\partial\beta^z}{\partial z} + 2\frac{\partial\beta^\varphi}{\partial\varphi} + 2\frac{\beta^R}{R}\right), \tag{A.11}$$

$$K^{Rz} = K^{zR} = \frac{1}{2\alpha}\left(\gamma^{RR}\frac{\partial\beta^z}{\partial R} + \gamma^{zz}\frac{\partial\beta^R}{\partial z}\right), \tag{A.12}$$

$$K^{R\varphi} = K^{\varphi R} = \frac{1}{2\alpha}\left(\gamma^{RR}\frac{\partial\beta^\varphi}{\partial R} + \gamma^{\varphi\varphi}\frac{\partial\beta^R}{\partial\varphi}\right), \tag{A.13}$$

$$K^{z\varphi} = K^{\varphi z} = \frac{1}{2\alpha}\left(\gamma^{zz}\frac{\partial\beta^\varphi}{\partial z} + \gamma^{\varphi\varphi}\frac{\partial\beta^z}{\partial\varphi}\right). \tag{A.14}$$

**Spherical Coordinate**

In this case, the line element $ds^2$ can be expressed as

$$ds^2 = \psi^4(dr^2 + d\theta^2 + r^2\sin^2\theta d\phi^2) \tag{A.15}$$

The non-vanishing extrinsic curvature $K_{ij}$ are:

$$K^{rr} = \frac{\gamma^{rr}}{3\alpha}\left(2\frac{\partial\beta^r}{\partial r} - \frac{\partial\beta^\theta}{\partial\theta} - \frac{\partial\beta^\phi}{\partial\phi} - \frac{2}{r}\beta^r - \cot\theta\beta^\theta\right) \tag{A.16}$$

$$K^{\theta\theta} = \frac{\gamma^{\theta\theta}}{3\alpha}\left(-\frac{\partial\beta^r}{\partial r} + 2\frac{\partial\beta^\theta}{\partial\theta} - \frac{\partial\beta^\phi}{\partial\phi} + \frac{\beta^r}{r} - \cot\theta\beta^\theta\right) \tag{A.17}$$

$$K^{\phi\phi} = \frac{\gamma^{\phi\phi}}{3\alpha}\left(-\frac{\partial\beta^r}{\partial r} - \frac{\partial\beta^\theta}{\partial\theta} + 2\frac{\partial\beta^\phi}{\partial\phi} + \frac{\beta^r}{r} + 2\cot\theta\beta^\theta\right) \tag{A.18}$$

$$K^{r\theta} = K^{\theta r} = \frac{1}{2\alpha}\left(\gamma^{rr}\frac{\partial\beta^\theta}{\partial r} + \gamma^{\theta\theta}\frac{\partial\beta^r}{\partial\theta}\right) \tag{A.19}$$

$$K^{r\phi} = K^{\phi r} = \frac{1}{2\alpha}\left(\gamma^{rr}\frac{\partial\beta^\phi}{\partial r} + \gamma^{\phi\phi}\frac{\partial\beta^r}{\partial\phi}\right) \tag{A.20}$$

$$K^{\theta\phi} = K^{\phi\theta} = \frac{1}{2\alpha}\left(\gamma^{\theta\theta}\frac{\partial\beta^\phi}{\partial\theta} + \gamma^{\phi\phi}\frac{\partial\beta^\theta}{\partial\phi}\right) \tag{A.21}$$

## A.2 Vectorial elliptic equations in xCFC scheme

As mentioned in section 2.5.2, instead of solving coordinate-basis components of the vector fields $X^i$ or $\beta^i$, the orthonormal-basis components for vector fields are solved in the vectorial elliptic equations (2.44) and (2.47). The expressions of these vectorial elliptic equations in orthonormal-basis form is non-trivial when we work in cylindrical coordinate or spherical coordinate. Here we list out the relations we implemented in `Gmunu`.

### Cylindrical coordinate

We rewrite a generic vector as

$$X^{\hat{R}} \equiv X^R, \qquad X^{\hat{z}} \equiv X^z, \qquad X^{\hat{\varphi}} \equiv RX^{\varphi}. \tag{A.22}$$

The conformal vector Laplacian (the left hand side of equations (2.44) and (2.47)) are

$$(\tilde{\Delta}\boldsymbol{X})^{\hat{R}} = \tilde{\Delta}X^{\hat{R}} - \frac{X^{\hat{R}}}{R^2} - \frac{2}{R^2}\frac{\partial X^{\hat{\varphi}}}{\partial\varphi} + \frac{1}{3}\frac{\partial}{\partial R}\left(\tilde{\nabla}_j X^j\right), \tag{A.23}$$

$$(\tilde{\Delta}\boldsymbol{X})^{\hat{z}} = \tilde{\Delta}X^{\hat{z}} + \frac{1}{3}\frac{\partial}{\partial z}\left(\tilde{\nabla}_j X^j\right), \tag{A.24}$$

$$(\tilde{\Delta}\boldsymbol{X})^{\hat{\varphi}} = \tilde{\Delta}X^{\hat{\varphi}} - \frac{X^{\hat{\varphi}}}{R^2} + \frac{2}{R^2}\frac{\partial X^{\hat{R}}}{\partial\varphi} + \frac{1}{3R}\frac{\partial}{\partial\varphi}\left(\tilde{\nabla}_j X^j\right), \tag{A.25}$$

where Laplacian of a scalar function $u(R, z, \varphi)$ is

$$\tilde{\Delta}u = \frac{1}{R}\frac{\partial}{\partial R}\left(R\frac{\partial u}{\partial R}\right) + \frac{\partial^2 u}{\partial z^2} + \frac{1}{R^2}\frac{\partial^2 u}{\partial\varphi^2}, \tag{A.26}$$

the divergence of the vector $\boldsymbol{X}$ is

$$\tilde{\nabla}_j X^j = \frac{\partial X^{\hat{R}}}{\partial R} + \frac{\partial X^{\hat{z}}}{\partial z} + \frac{1}{R}\frac{\partial X^{\hat{\varphi}}}{\partial\varphi} + \frac{X^{\hat{R}}}{R}, \tag{A.27}$$

and

$$\frac{\partial}{\partial R}\left(\tilde{\nabla}_j X^j\right) = \frac{\partial^2 X^{\hat{R}}}{\partial R^2} + \frac{\partial^2 X^{\hat{z}}}{\partial R\partial z} + \frac{\partial^2 X^{\hat{\varphi}}}{\partial R\partial\varphi} - \frac{1}{R^2}\frac{\partial X^{\hat{\varphi}}}{\partial\varphi} + \frac{1}{R}\frac{\partial X^{\hat{R}}}{\partial R} - \frac{X^{\hat{R}}}{R^2}, \tag{A.28}$$

$$\frac{\partial}{\partial z}\left(\tilde{\nabla}_j X^j\right) = \frac{\partial}{\partial z}\left(\frac{\partial X^{\hat{R}}}{\partial R} + \frac{\partial X^{\hat{z}}}{\partial z} + \frac{\partial X^{\hat{\varphi}}}{\partial\varphi}\right) + \frac{1}{R}\frac{\partial X^{\hat{R}}}{\partial z}, \tag{A.29}$$

$$\frac{\partial}{\partial\varphi}\left(\tilde{\nabla}_j X^j\right) = \frac{\partial}{\partial\varphi}\left(\frac{\partial X^{\hat{R}}}{\partial R} + \frac{\partial X^{\hat{z}}}{\partial z} + \frac{\partial X^{\hat{\varphi}}}{\partial\varphi}\right) + \frac{1}{R}\frac{\partial X^{\hat{R}}}{\partial\varphi}. \tag{A.30}$$

### Spherical coordinate

We rewrite a generic vector as

$$X^{\hat{r}} \equiv X^r, \qquad X^{\hat{\theta}} \equiv rX^{\theta}, \qquad X^{\hat{\phi}} \equiv r\sin\theta X^{\phi}. \tag{A.31}$$

The conformal vector Laplacian (the left hand side of equations (2.44) and (2.47)) are

$$(\tilde{\Delta}\boldsymbol{X})^{\hat{r}} = \tilde{\Delta}X^{\hat{r}} - \frac{2}{r^2}\left[X^{\hat{r}} + \frac{1}{\sin\theta}\frac{\partial}{\partial\theta}\left(\sin\theta X^{\hat{\theta}}\right) + \frac{1}{\sin\theta}\frac{\partial X^{\hat{\phi}}}{\partial\phi}\right] + \frac{1}{3}\frac{\partial}{\partial r}\left(\tilde{\nabla}_j X^j\right), \tag{A.32}$$

$$(\tilde{\Delta}\boldsymbol{X})^{\hat{\theta}} = \tilde{\Delta}X^{\hat{\theta}} + \frac{2}{r^2}\frac{\partial X^{\hat{r}}}{\partial\theta} - \frac{X^{\hat{\theta}}}{r^2\sin^2\theta} - \frac{2\cos\theta}{r^2\sin^2\theta}\frac{\partial X^{\hat{\phi}}}{\partial\phi} + \frac{1}{3r}\frac{\partial}{\partial\theta}\left(\tilde{\nabla}_j X^j\right), \tag{A.33}$$

$$(\tilde{\Delta}\boldsymbol{X})^{\hat{\phi}} = \tilde{\Delta}X^{\hat{\phi}} - \frac{X^{\hat{\phi}}}{r^2\sin^2\theta} + \frac{2}{r^2\sin\theta}\frac{\partial X^{\hat{r}}}{\partial\phi} + \frac{2\cos\theta}{r^2\sin^2\theta}\frac{\partial X^{\hat{\theta}}}{\partial\phi} + \frac{1}{3r\sin\theta}\frac{\partial}{\partial\phi}\left(\tilde{\nabla}_j X^j\right), \tag{A.34}$$

where the Laplacian of a scalar function $u(r,\theta,\phi)$ is

$$\tilde{\Delta}u = \frac{1}{r^2}\frac{\partial}{\partial r}\left(r^2\frac{\partial u}{\partial r}\right) + \frac{1}{r^2\sin\theta}\frac{\partial}{\partial\theta}\left(\sin\theta\frac{\partial u}{\partial\theta}\right) + \frac{1}{r^2\sin^2\theta}\frac{\partial^2 u}{\partial\phi^2}, \tag{A.35}$$

the divergence of the vector $\boldsymbol{X}$ is

$$\tilde{\nabla}_j X^j = \frac{1}{r^2}\frac{\partial}{\partial r}\left(r^2 X^{\hat{r}}\right) + \frac{1}{r\sin\theta}\frac{\partial}{\partial\theta}\left(\sin\theta X^{\hat{\theta}}\right) + \frac{1}{r\sin\theta}\frac{\partial X^{\hat{\phi}}}{\partial\phi}, \tag{A.36}$$

and

$$\begin{aligned}\frac{\partial}{\partial r}\left(\tilde{\nabla}_j X^j\right) = \frac{1}{r^2\sin^2\theta}\Bigg\{ &\sin^2\theta\left[\frac{\partial}{\partial r}\left(r^2\frac{\partial X^{\hat{r}}}{\partial r}\right) - 2X^{\hat{r}} - \frac{\partial X^{\hat{\theta}}}{\partial\theta} + r\frac{\partial^2 X^{\hat{\theta}}}{\partial r\partial\theta}\right] \\ &+ \sin\theta\left[\cos\theta\left(r\frac{\partial X^{\hat{\theta}}}{\partial r} - X^{\hat{\theta}}\right) - \frac{\partial X^{\hat{\theta}}}{\partial\phi} + r\frac{\partial^2 X^{\hat{\phi}}}{\partial r\partial\phi}\right]\Bigg\},\end{aligned} \tag{A.37}$$

$$\begin{aligned}\frac{\partial}{\partial\theta}\left(\tilde{\nabla}_j X^j\right) = \frac{r}{r^2\sin^2\theta}\Bigg\{ &\sin^2\theta\left[r\frac{\partial^2 X^{\hat{r}}}{\partial\theta\partial r} + 2\frac{\partial X^{\hat{r}}}{\partial\theta}\right] - X^{\hat{\theta}} - \cos\theta\frac{\partial X^{\hat{\phi}}}{\partial\phi} \\ &+ \sin\theta\left[\frac{\partial}{\partial\theta}\left(\sin\theta\frac{\partial X^{\hat{\theta}}}{\partial\theta}\right) + \frac{\partial^2 X^{\hat{\phi}}}{\partial\theta\partial\phi}\right]\Bigg\},\end{aligned} \tag{A.38}$$

$$\frac{\partial}{\partial\phi}\left(\tilde{\nabla}_j X^j\right) = \frac{r\sin\theta}{r^2\sin^2\theta}\left\{\sin\theta\left[r\frac{\partial^2 X^{\hat{r}}}{\partial\phi\partial r} + 2\frac{\partial X^{\hat{r}}}{\partial\phi} + \frac{\partial^2 X^{\hat{\theta}}}{\partial\theta\partial\phi}\right] + \cos\theta\frac{\partial X^{\hat{\theta}}}{\partial\phi} + \frac{\partial^2 X^{\hat{\phi}}}{\partial^2\phi}\right\}. \tag{A.39}$$

# Appendix B

# Reference flat metric in 3D

The cell volume $\Delta V$, cell surface $\Delta A$ and the volume-average of the 3-Christoffel symbols $\left\langle \hat{\Gamma}^l_{ik} \right\rangle$ which is contained in the geometrical are non-trivial when the reference metric $\hat{\gamma}_{ij}$ is chosen to be cylindrical or spherical. Here we list out the relations we implemented in `Gmunu`.

## Cylindrical Coordinate

The line element can be expressed as: $ds^2 = dR^2 + dz^2 + R^2 d\varphi^2$, with the reference metric $\hat{\gamma}_{ij}$:

$$\hat{\gamma}_{ij} = \begin{bmatrix} 1 & 0 & 0 \\ 0 & 1 & 0 \\ 0 & 0 & R^2 \end{bmatrix}. \tag{B.1}$$

The associated 3-Christoffel symbols $\hat{\Gamma}^l_{ik}$ are:

$$\hat{\Gamma}^R_{ij} = \begin{bmatrix} 0 & 0 & 0 \\ 0 & 0 & 0 \\ 0 & 0 & -R \end{bmatrix}, \qquad \hat{\Gamma}^z_{ij} = \begin{bmatrix} 0 & 0 & 0 \\ 0 & 0 & 0 \\ 0 & 0 & 0 \end{bmatrix}, \qquad \hat{\Gamma}^\varphi_{ij} = \begin{bmatrix} 0 & 0 & \frac{1}{R} \\ 0 & 0 & 0 \\ \frac{1}{R} & 0 & 0 \end{bmatrix}. \tag{B.2}$$

The geometrical source terms for the momentum equations are:

$$\hat{\Gamma}^l_{Rk}(f_{S_l})^k = \hat{\Gamma}^\varphi_{R\varphi}(f_{S_\varphi})^\varphi, \tag{B.3}$$

$$\hat{\Gamma}^l_{zk}(f_{S_l})^k = 0, \tag{B.4}$$

$$\hat{\Gamma}^l_{\varphi k}(f_{S_l})^k = 0. \tag{B.5}$$

Here we note that since $z$ and $\varphi$ do not explicitly enter into the reference metric $\hat{\gamma}_{ij}$, the corresponding geometrical source terms for the momentum equation $q_{S_j}$ are vanishing. In this formulations, the linear momentum $q_{S_z}$ and the angular momentum $q_{S_\varphi}$ are conserved to machine precision.

To work out the cell volume $\Delta V$, cell surface $\Delta A$ and the volume-average of the 3-Christoffel symbols $\left\langle \hat{\Gamma}^l_{ik} \right\rangle$, we define the following notations:

$$R_\pm \equiv R \pm \frac{1}{2}\Delta R, \qquad z_\pm \equiv z \pm \frac{1}{2}\Delta z, \qquad \varphi_\pm \equiv \varphi \pm \frac{1}{2}\Delta\varphi, \tag{B.6}$$

where $(R, z, \varphi)$ are the location at the cell centre at some particular point while $(\Delta R, \Delta z, \Delta\varphi)$ are the corresponding grid sizes. The cell surface $\Delta A$ and the cell volume $\Delta V$ can then be expressed as:

$$\Delta l_R = R\,(\Delta R)\,, \tag{B.7}$$
$$\Delta l_z = R\,(\Delta z)\,, \tag{B.8}$$
$$\Delta l_\varphi = R\,(\Delta\varphi)\,, \tag{B.9}$$
$$\Delta A_R\Big|_{R_\pm} = \left(R \pm \frac{\Delta R}{2}\right)(\Delta z)\,(\Delta\varphi)\,, \tag{B.10}$$
$$\Delta A_z\Big|_{z_\pm} = R\,(\Delta R)\,(\Delta\varphi)\,, \tag{B.11}$$
$$\Delta A_\varphi\Big|_{\varphi_\pm} = R\,(\Delta R)\,(\Delta z)\,, \tag{B.12}$$
$$\Delta V = R\,(\Delta R)\,(\Delta z)\,(\Delta\varphi)\,. \tag{B.13}$$

Finally, the non-vanishing volume-averaged 3-Christoffel symbols $\left\langle \hat{\Gamma}^l_{ik} \right\rangle$ are:

$$\left\langle \hat{\Gamma}^R_{\varphi\varphi} \right\rangle = -\frac{1}{R}\left(R^2 + \frac{1}{12}\,(\Delta R)^2\right), \tag{B.14}$$
$$\left\langle \hat{\Gamma}^\varphi_{\varphi R} \right\rangle = \left\langle \hat{\Gamma}^\varphi_{R\varphi} \right\rangle = \frac{1}{R}. \tag{B.15}$$

## Spherical Coordinate

The line element can be expressed as: $ds^2 = dr^2 + r^2 d\theta^2 + r^2 \sin^2\theta d\phi^2$, with the reference metric $\hat{\gamma}_{ij}$:

$$\hat{\gamma}_{ij} = \begin{bmatrix} 1 & 0 & 0 \\ 0 & r^2 & 0 \\ 0 & 0 & r^2\sin^2\theta \end{bmatrix}. \tag{B.16}$$

The associated 3-Christoffel symbols $\hat{\Gamma}^l_{ik}$ are:

$$\hat{\Gamma}^r_{ij} = \begin{bmatrix} 0 & 0 & 0 \\ 0 & -r & 0 \\ 0 & 0 & -r\sin^2\theta \end{bmatrix}, \tag{B.17}$$
$$\hat{\Gamma}^\theta_{ij} = \begin{bmatrix} 0 & \frac{1}{r} & 0 \\ \frac{1}{r} & 0 & 0 \\ 0 & 0 & -\sin\theta\cos\theta \end{bmatrix}, \tag{B.18}$$
$$\hat{\Gamma}^\phi_{ij} = \begin{bmatrix} 0 & 0 & \frac{1}{r} \\ 0 & 0 & \cot\theta \\ \frac{1}{r} & \cot\theta & 0 \end{bmatrix}. \tag{B.19}$$

The geometrical source terms for the momentum equations are:

$$\hat{\Gamma}^l_{rk}(f_{S_l})^k = \hat{\Gamma}^\theta_{r\theta}(f_{S_\theta})^\theta + \hat{\Gamma}^\phi_{r\phi}(f_{S_\phi})^\phi, \tag{B.20}$$
$$\hat{\Gamma}^l_{\theta k}(f_{S_l})^k = \hat{\Gamma}^r_{\theta\theta}(f_{S_r})^\theta + \hat{\Gamma}^\theta_{\theta r}(f_{S_\theta})^r + \hat{\Gamma}^\phi_{\theta\phi}(f_{S_\phi})^\phi, \tag{B.21}$$
$$\hat{\Gamma}^l_{\phi k}(f_{S_l})^k = 0. \tag{B.22}$$

Simularity, as in the cylindrical case, the angular momentum $q_{S_\phi}$ are conserved to machine precision.

To work out the cell volume $\Delta V$, cell surface $\Delta A$ and the volume-average of the 3-Christoffel symbols $\left\langle \hat{\Gamma}^l_{ik} \right\rangle$, we define the following notations:

$$r_\pm = r \pm \frac{1}{2}\Delta r, \qquad \theta_\pm = \theta \pm \frac{1}{2}\Delta\theta, \qquad \phi_\pm = \phi \pm \frac{1}{2}\Delta\phi, \tag{B.23}$$

where $(r, \theta, \phi)$ are the location at the cell centre at some particular point while $(\Delta r, \Delta\theta, \Delta\phi)$ are the corresponding grid sizes. The cell surface $\Delta A$ and the cell volume $\Delta V$ can then be expressed as:

$$\Delta l_r = \left( \left( r^2 + \frac{1}{12}(\Delta r)^2 \right) \Delta r \right) \sin\theta \tag{B.24}$$

$$\Delta l_\theta = r^2 \left( 2\sin\theta \sin\left( \frac{\Delta\theta}{2} \right) \right) \tag{B.25}$$

$$\Delta l_\phi = r^2 \sin\theta \, (\Delta\phi) \tag{B.26}$$

$$\Delta A_r\Big|_{r_\pm} = \left( r \pm \frac{\Delta r}{2} \right)^2 \left( 2\sin\theta \sin\left( \frac{\Delta\theta}{2} \right) \right) (\Delta\phi) \tag{B.27}$$

$$\Delta A_\theta\Big|_{\theta_\pm} = \left( \left( r^2 + \frac{1}{12}(\Delta r)^2 \right) \Delta r \right) \left( \sin\left( \theta \pm \frac{\Delta\theta}{2} \right) \right) (\Delta\phi) \tag{B.28}$$

$$\Delta A_\phi\Big|_{\phi_\pm} = \left( \left( r^2 + \frac{1}{12}(\Delta r)^2 \right) \Delta r \right) \left( 2\sin\theta \sin\left( \frac{\Delta\theta}{2} \right) \right) \tag{B.29}$$

$$\Delta V = \left( \left( r^2 + \frac{1}{12}(\Delta r)^2 \right) \Delta r \right) \left( 2\sin\theta \sin\left( \frac{\Delta\theta}{2} \right) \right) (\Delta\phi) \tag{B.30}$$

Finally, the non-vanishing volume-averaged 3-Christoffel symbols $\left\langle \hat{\Gamma}^l_{ik} \right\rangle$ are:

$$\left\langle \hat{\Gamma}^\theta_{r\theta} \right\rangle = \left\langle \hat{\Gamma}^\theta_{\theta r} \right\rangle = \left\langle \hat{\Gamma}^\phi_{r\phi} \right\rangle = \left\langle \hat{\Gamma}^\phi_{\phi r} \right\rangle = \frac{1}{\Delta V}\frac{1}{2}\left( \Delta A_r\Big|_{r_+} - \Delta A_r\Big|_{r_-} \right) \tag{B.31}$$

$$\left\langle \hat{\Gamma}^r_{\theta\theta} \right\rangle = -\frac{1}{\Delta V}\frac{1}{4}\left( r_+^2 \Delta A_r\Big|_{r_+} - r_-^2 \Delta A_r\Big|_{r_-} \right) \tag{B.32}$$

$$\left\langle \hat{\Gamma}^r_{\phi\phi} \right\rangle = \frac{1}{\Delta V}\left( -\frac{1}{4} r^4 \Big|_{r_-}^{r^+} \right) \left( \frac{1}{3}\cos^3\theta - \cos\theta \right) \Big|_{\theta_-}^{\theta^+} \Delta\phi \tag{B.33}$$

$$\left\langle \hat{\Gamma}^\theta_{\phi\phi} \right\rangle = -\frac{1}{3}\frac{1}{\Delta V}\left( \sin^2(\theta_+)\Delta A_\theta\Big|_{\theta_+} - \sin^2(\theta_-)\Delta A_\theta\Big|_{\theta_-} \right) \tag{B.34}$$

$$\left\langle \hat{\Gamma}^\phi_{\theta\phi} \right\rangle = \left\langle \hat{\Gamma}^\phi_{\phi\theta} \right\rangle = \cot\theta \tag{B.35}$$

# Appendix C

# Numerical methods for solving Fermi integrals

## C.1 Fermi integrals of integer order

## C.2 Fermi integrals of half-integer order

# Appendix D

# Hydrodynamics equations with neutrino source terms